Regional Studies in Marine Science 32 (2019) 100809

Contents lists available at ScienceDirect

Regional Studies in Marine Science

journal homepage: www.elsevier.com/locate/rsma

Morphological plasticity in a Fijian Seagrass: *Halophila ovalis* subsp. *bullosa*

Shalini Singh [a,d,*], Paul C. Southgate [b], Monal M. Lal [b,c]

[a] Pacific Centre for Environment and Sustainable Development, University of the South Pacific, Lower Laucala Campus, Laucala Bay Road, Suva, Fiji
[b] Australian Centre for Pacific Islands Research, School of Science and Engineering, University of the Sunshine Coast, Maroochydore, Queensland 4558, Queensland, Australia
[c] School of Marine Studies, Faculty of Science, Technology and Environment, University of the South Pacific, Lower Laucala Campus, Laucala Bay Road, Suva, Fiji
[d] College of Agriculture, Fisheries and Forestry, Fiji National University, Koronivia, Nausori, Fiji

ARTICLE INFO

Article history:
Received 5 December 2018
Received in revised form 14 August 2019
Accepted 22 August 2019
Available online 26 August 2019

Keywords:
DNA barcoding
Seagrass
Halophila
Nuclear marker
Chloroplast marker
Taxonomic identification

ABSTRACT

Seagrasses are marine flowering plants found along both tropical and temperate coastlines; they possess great ecological importance as nurseries, nutrient sinks, and providers of critical marine habitat. Understanding the distribution and diversity of seagrass habitats is important for their conservation and management, however this is impeded by varying species' diversity, the extensive distribution of seagrasses and taxonomic uncertainty. In the Fiji Islands, the tropical seagrass *Halophila ovalis* and its subspecies *H. ovalis bullosa* are the subject of taxonomic controversy, as a singular morphological characteristic distinguishes the two. This characteristic is the bullated, or blister-like leaves of the latter, compared to the smooth leaves of the former, which in some instances have been observed on the same plant (S.S., *pers. obs.*). This study examined material from both taxa, along with three other seagrass species (*Halodule pinifolia*, *H. uninervis* and *Syringodium isoetifolium*; total $n = 95$) and used independent morphological and molecular barcoding approaches to assess the conspecificity of the two *Halophila* taxa. Examination of vegetative and reproductive characters was not able to distinguish between *H. ovalis* and *H. ovalis* subsp. *bullosa*, while phylogenetic reconstructions using ITS2, *matK* and *trnH-psbA* barcodes supported their monophyly. We recommend revision and merger of these taxa, while the approach used here is highly useful for taxonomic resolution in other seagrass taxa, for their conservation, restoration and management.

© 2019 Elsevier B.V. All rights reserved.

1. Introduction

Seagrasses are marine flowering plants with a wide global distribution along both tropical and temperate coastlines (den Hartog and Kuo, 2006; Short et al., 2007). Collectively, seagrasses possess great ecological importance, as they support high levels of biodiversity, play important roles in fisheries, provide nursing grounds, stabilise coastal sediments, facilitate nutrient cycling, act as carbon sinks and reservoirs, and provide many other ecosystem functions (Short et al., 2007). While seagrass species diversity is low compared to other marine taxa (<60 species described), species' ranges can be highly extensive, covering several thousands of kilometres of coastal habitat (Short et al., 2007; Waycott et al., 2006).

Investigating worldwide seagrass distribution and diversity is an important first step in understanding these complex habitats, which permits geographical comparisons of seagrass ecology, evolution, and taxonomy. Such comparisons allow evaluation of past and present human-mediated impacts on seagrass ecosystems, and may reveal insights into conservation measures for their future protection (Short et al., 2007). However, the extensive distribution of seagrasses, varying species diversity patterns and widespread areas of undocumented seagrass habitat, all present challenges for investigating species' ranges, ecology and taxonomy (Short et al., 2007; Waycott et al., 2006).

In addition to these impediments, ecological studies of seagrasses can be confounded by taxonomic uncertainty. Despite seagrasses representing less than 0.1% of all known angiosperm taxa, the taxonomic status of some species remains unclear, with high morphological similarity within certain groups of taxa contributing to this (Vanitha et al., 2016). For a few taxa, convergent morphology has been documented (Waycott et al., 2006), which along with morphological plasticity (Maxwell et al., 2014; McDonald et al., 2016), can render species identification using

* Corresponding author at: Pacific Centre for Environment and Sustainable Development, University of the South Pacific, Lower Laucala Campus, Laucala Bay Road, Suva, Fiji.
E-mail address: sophie.shalinisingh@gmail.com (S. Singh).

https://doi.org/10.1016/j.rsma.2019.100809
2352-4855/© 2019 Elsevier B.V. All rights reserved.

traditional phenotypic characters alone ineffective, or highly challenging. The use of molecular information, such as DNA barcoding genes have been used to resolve taxonomic relationships in several seagrass taxa (den Hartog and Kuo, 2006; Waycott et al., 2002), and when combined with phenotypic information (Ji et al., 2013; Cowart et al., 2015; Trivedi et al., 2016), can potentially resolve previously confounded species-level relationships.

An example of a seagrass group possessing uncertain taxonomy is the genus *Halophila* (Thouars), which contains approximately 21 species and comprises five sections. Species within this genus are currently described on the basis of morphological differences (den Hartog and Kuo, 2006; Kuo et al., 2006; Short et al., 2011; Kim et al., 2017). However, similarities in morphological characters and subtle irregularities between published species and sub-species descriptions have raised questions on the validity of these relationships (den Hartog and Kuo, 2006; Kim et al., 2017). In the Fiji Islands, five species of seagrass from two families (Hydrocharitaceae and Cymodoceaceae) have been described, including *Halophila ovalis*, and its subspecies *H. ovalis bullosa* (Skelton and South, 2006; McKenzie and Yoshida, 2007; Tuiwawa et al., 2014).

Halophila ovalis presents an interesting study subject among tropical seagrasses, as the species has a wide Indo-Pacific distribution, ranging from East Africa to the western Pacific, while its subspecies *H. ovalis bullosa* is much more range-restricted, being endemic to Fiji, Tonga and Samoa (Tuiwawa et al., 2014). While Tuiwawa et al. (2014) and Skelton and South (2006) described morphological characters to identify *H. ovalis*, the primary differentiating character between this taxon and its subspecies *H. ovalis bullosa* remain the bullations (blisters or pucker-like structures) present on the leaf blades, compared to the smooth blades of the former. During field collections for this study, several specimens of *H. ovalis* were observed to possess both smooth and bullated leaves (Shalini Singh, *pers. obs.*). Similar observations have been recorded previously in literature, where experimental manipulations were able to induce bullate-leaved plants to produce smooth leaves, and vice versa, suggesting that environmental factors may play a role in the expression of this phenotype (McMillan and Bridges, 1982; Skelton and South, 2006).

These observations suggest that *H. ovalis* possesses phenotypic plasticity (Maxwell et al., 2014; McDonald et al., 2016), and given that discrimination between it and *H. ovalis* subsp. *bullosa* is based largely on a single morphological feature, recognition of the latter as a distinct taxon requires further investigation. This study addresses the taxonomic identities of *H. ovalis* and its subspecies *H. ovalis bullosa* from the Fiji Islands using independent morphological and molecular barcoding approaches (Ji et al., 2013; Cowart et al., 2015; Trivedi et al., 2016). Both vegetative and reproductive morphological characters were examined, and together with two barcoding genes, used to resolve if Fijian *H. ovalis* and *H. ovalis* subsp. *bullosa* are in fact conspecific. This investigation is the first of its kind to employ complementary morphological and molecular approaches to examine Fijian seagrass material, and the findings generated have high utility for resolving uncertain taxonomy in other aquatic plant taxa, and for informing global seagrass conservation and management efforts.

2. Methodology

2.1. Study area

The Fiji Islands are located in the southwest Pacific Ocean between the latitudes of 15° to 22°S and longitude 177°W to 174°E. Fiji consists of more than 332 islands, most of which are volcanic, and about 100 are inhabited, covering a total land area of 18,376 km^2 and an exclusive economic zone of 1.3 million km^2. The two major islands are Viti Levu and Vanua Levu, with the weather marked by a wet/warm season from October to March, and a cool/dry season from April to September. The climate of Fiji is generally categorised as an oceanic tropical marine climate, averaging 26 °C with annual rainfall ranging from 1800 to 2600 mm. The major features that drive Fiji's climate are the El Nino Southern Oscillation (ENSO) phenomenon that occurs every four years on average, the South Pacific Convergence Zone and the Trade Winds (see Fig. 1).

2.2. Seagrass tissue sampling, collection and morphometric analyses

Seagrass samples (total n = 95) were collected from July to September 2017 at 22 coastal sites in the Fiji Islands by wading in the intertidal zone. These included *H. uninervis* (n = 21), *H. pinifolia* (n = 20), *H. ovalis* (n = 15), *H. ovalis* subsp. *bullosa* (n = 21) and *S. isoetifolium* (n = 18). Leaf morphometric analyses were conducted on 15 leaves from different leaf pairs collected randomly across the seagrass bed at each collection site. Reproductive shoots (including female and male flowers, and fruits) were also collected from Nasese (site 1) and Hilton Denarau (site 18), which were counted and measured. Field identification to species level was made using the taxonomic keys of Tuiwawa et al. (2014) and the Seagrass-Watch field guide (McKenzie and Yoshida, 2007). Seagrass-Watch is a global scientific, non-destructive, seagrass assessment and monitoring program (http://www.seagrasswatch.org).

At each site, 3–5 whole plant samples were collected at random from each of the taxa present. In general, the seagrasses were dug out, cleaned in seawater to remove accompanying debris, and transported in labelled Ziploc® plastic bags to the laboratory. Epiphytes such as coralline algae adhering to both sides of the seagrass leaves were removed by gentle scraping using a microscope slide, and samples washed in clean freshwater. Although whole plants were taken, only the leaf fragments were immediately placed into labelled Ziploc® plastic bags containing silica gel desiccant and stored at room temperature until use.

Sites were mapped in the field with a handheld Global Positioning System (GPS) unit (Garmin *eTrex10*). To ensure that specimen records from each specimen was traceable, sample collection data including GPS coordinates, taxonomic information and photographic images recorded during field collections were uploaded to the Barcoding of Life Data (BOLD) system repository (http://www.boldsystems.org), (Ratnasingham and Hebert, 2007, 2013). This enabled the provision of support for identifications, and permitted easier comparisons between species, as per Kuzmina et al. (2017).

2.3. DNA extraction, amplification, sequencing and sequence editing

Silica gel-dried leaf tissue (1 × 0.5 cm size) from each sample were transferred into 96 well-microplates (250 μL, semi-skirted; Eppendorf, Hamburg, Germany), and submitted to the Canadian Centre for DNA Barcoding (CCDB) in Guelph, Ontario, Canada, for genotyping under the BOLD system (http://www.boldsystems.org), (Ratnasingham and Hebert, 2007, 2013). At CCDB, the leaf tissue samples were processed for genomic DNA (gDNA) extraction using a semi-automated glass fibre plate DNA extraction protocol (Ivanova et al., 2006, 2008; Whitlock et al., 2008).

Briefly, approximately 1–5 mg of dried leaf tissue was pulverised using a TissueLyser II (Qiagen, Germantown, Maryland, USA) homogeniser, and the Axygen Mini Tube System (Axygen Scientific, Union City, California, USA), as per Kuzmina et al. (2017). A single 3.17 mm stainless steel bead was used per tube, and disruption was carried out at 28 Hz for 60–90 s at room

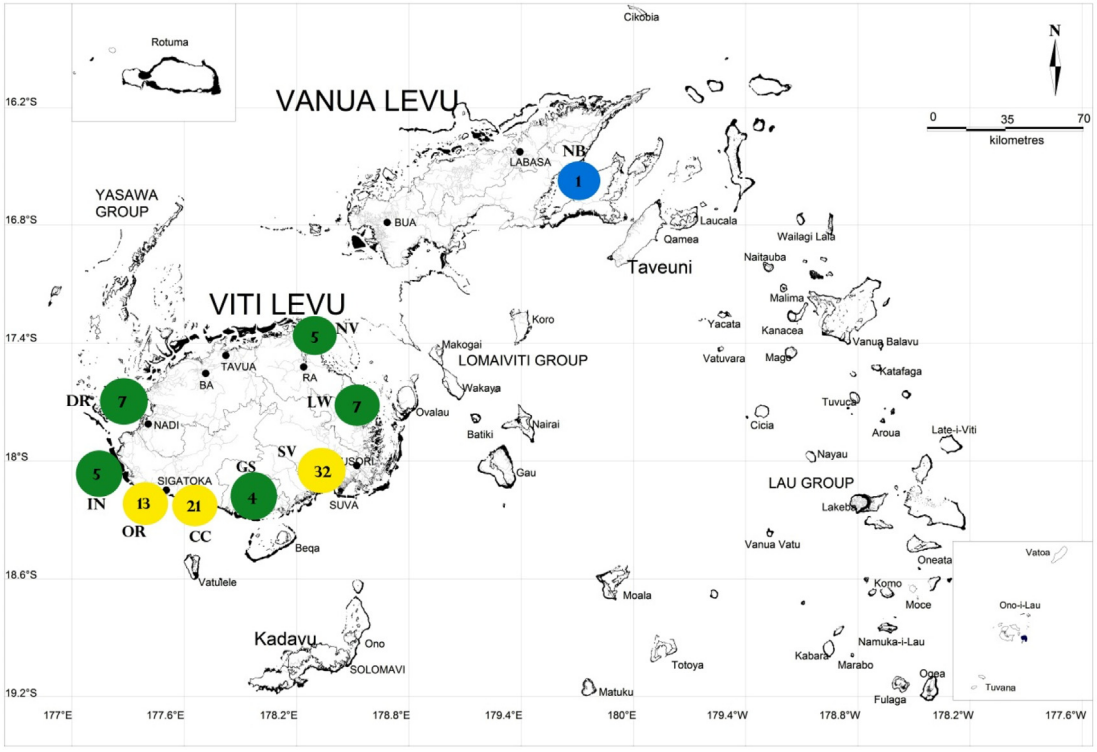

Fig. 1. Map of sampling locations of Hydrocharitaceae and Cymodoceaceae seagrass meadows along the coastlines in the Fiji Islands. Coastal outlines are presented in black and 95 sampling site GPS point clusters are shown by circles. Colour codes of circles represent the following: blue represents a single GPS point; green represents more than 1 point and yellow represents more than 10 points. Numbers presented within the circles indicate the sample sizes of seagrass specimens collected and used in phylogenetic analyses. Sampling site codes represent the following locations: NB, Natewa Bay, Labasa; NV, Navolau village, Rakiraki; LW, Lawaki village, Tailevu; SV, My Suva Park, Suva; GS, Fisheries Galoa station, Navua; CC, site at Coral coast, Sigatoka; OR, site at Outrigger reef, Sigatoka; IN, Intercontinental Natadola, Sigatoka; DR, Denarau Island, Nadi. (For interpretation of the references to colour in this figure legend, the reader is referred to the web version of this article.)
Source: The map base layer has been adapted from Lal et al. (2016).

temperature. Cell lysis was implemented using 2× cetyltrimethylammonium bromide (CTAB) buffer (250–400 μL), and the lysate incubated at 65 °C for 60–90 min, following which 50 μL volumes per sample were transferred to 96-well microplates with a Liquidator 96 (Mettler Toledo, Mississauga, Ontario, Canada) robotic liquid handler (Kuzmina et al., 2017). On a Biomek FX Workstation (Beckman Coulter, Mississauga, Ontario, Canada), gDNA was isolated and purified by binding to glass fibre filtration columns (Ivanova et al., 2008; Kuzmina et al., 2017).

Sequences in the internal transcribed spacer (ITS2) region of nuclear ribosomal DNA (nrDNA), together with the maturase K (*matK*) plastid gene and *trnH-psbA* intergenic spacer region (cpDNA) were amplified via PCR as per Kuzmina and Ivanova (2011a,b) and Kuzmina et al. (2017). The primer pairs used for targeting these regions were as follows. ITS2: ITS-S2F(20/20bp) (Chen et al., 2010) (3′-ATGCGATACTTGGTGTGAAT-5′) with ITS4 (White et al., 1990) (5′-TCCTCCGCTTATTGATATGC-3′); *matK*: matK-xf (Ford et al., 2009) (3′-TAATTTACGATCAATTCATTC-5′) with matKMALP(21/18bp) (Dunning and Savolainen, 2010) (5′-ACAAGAAAGTCGAAGTAT-3′); and *trnH-psbA*: psbA3_f(21/22bp) (Sang et al., 1997) (3′-GTTATGCATGAACGTAATGCT-5′) with trnHf_05 (Tate and Simpson, 2003) (5′-CGCGCATGGTGGATT CACAATC-3′).

All PCR amplification was carried out on a Vapo.protect Mastercycler® pro S (Eppendorf, Hamburg, Germany) thermal cycler, with PCR cocktail mixes as described by Kuzmina et al. (2017). Platinum DNA Polymerase (Invitrogen) was used for amplification of the ITS2 region in all samples, under the following cycling conditions: 94 °C for 5 min; 35 cycles of 94 °C for 30 s, 56 °C for 30 s, 72 °C for 45 s, and a final extension step at 72 °C for 10 min. Phusion High Fidelity DNA Polymerase (Thermo Fisher) was used for the *matK* and *trnH-psbA* regions, with the following cycling conditions for the former: 98 °C for 45 s; 35 cycles of 98 °C for 10 s, 54 °C for 30 s, 72 °C for 40 s, and final extension at 72 °C for 10 min. For the latter, cycling conditions were 98 °C for 45 s; 35 cycles of 98 °C for 10 s, 64 °C for 30 s, 72 °C for 40 s, and final extension at 72 °C for 10 min. Following PCR, amplified products were cleaned and sequenced on an ABI 3730*xl* DNA Analyzer (Applied Biosystems, Foster City, California, USA), following standard manufacturer's procedures.

Chromatograms obtained post-sequencing were edited using CodonCode Aligner versions 3.7.1–6.0.2 (CodonCode Co., Centerville, Massachusetts, USA), with MUltiple Sequence Comparison by Log-Expectation (MUSCLE) alignments and BLASTn searches used to remove primer sequences, contaminant sequences and sequencing errors as per Kuzmina et al. (2017). Cleaned, filtered and edited sequences were then uploaded to the BOLD repository (www.boldsystems.org) for subsequent phylogenetic analyses.

2.4. Phylogenetic analyses

2.4.1. Model testing and selection

Nucleotide sequence analyses were performed in the MEGA6 package (Tamura et al., 2013), to edit sequences and perform alignments. Gaps in the sequences were treated as missing data, and final alignments for sequences in each of the three gene regions was by MUSCLE (Edgar, 2004). Aligned sequences for each region was then subjected to substitution model testing in the jModelTest package (Posada, 2008). Following calculation of likelihood scores as per the jModelTest manual, Bayesian Information

Criterion (BIC) scores including the negative log likelihood (-lnL) and BIC difference (delta parameter), were used to select the optimal model for use in phylogenetic inference. Reconstructions were carried out using both Bayesian and Maximum Likelihood (ML) methods.

2.5. Phylogenetic reconstruction

2.5.1. BayesIan reconstructions

Bayesian inference of phylogenetic relationships was carried out for all three data sets, with the MrBayes v3.2 package (Huelsenbeck and Ronquist, 2001; Ronquist and Huelsenbeck, 2003; Ronquist et al., 2012). Parameter settings were selected following test runs, and the appropriate substitution model selection determined using earlier jModelTest results.

For the *matK* sequences, because there is no direct implementation for the selected TPM1uf substitution model in MrBayes (see results), the analogous K81uf+G model as per Kimura (1981) and Lecocq et al. (2013) was utilised. The inputs for the data block were then set as follows: lset applyto=(all), nst = 6, rates = gamma; prset applyto = (all), revmatpr = dirichlet (1,1,1,1,1,1), statefreqpr = fixed(equal), shapepr = uniform (0.1,50) and pinvarpr = uniform (0,1). The selected models for the ITS2 and *trnH-psbA* regions are supported by MrBayes, and therefore standard inputs were used for these datasets.

Each analysis incorporated two runs of 100,000,000, 2,900,000 and 3,100,000 generations, for the ITS2, *matK* and *trnH-psbA* regions, respectively. Each run comprised 4 independent chains, with a temperature of 0.10 set for the heated chains, sampling frequency of 1000 and burn-in fraction of 20%. The burn-in threshold was selected on the basis that both independent runs had achieved convergence (*i.e.* stable log likelihood values reached for all sampled trees, gauged by the average standard deviation of split frequencies <0.01). Convergence was also independently assessed using Tracer v.1.6 (Rambaut et al., 2003).

The final trees for the Bayesian analysis were generated by selecting only those post-burn in trees found with the highest individual (p) and cumulative posterior (P) probabilities during Markov Chain Monte Carlo (MCMC) computations. These criteria varied between datasets, with the respective thresholds for the ITS2, *matK* and *trnH-psbA* datasets being $p = 0.000$, $P \geq 0.990$; $p = 0.000$, $P \geq 0.980$ and $p = 0.000$, $P \geq 0.980$, respectively. Consensus trees were then constructed from the final credible sets of trees using the strict consensus rule in the Dendroscope 3.5.7 package (Huson et al., 2007). All phylograms were visualised, inspected and edited in FigTree v.1.4.2 (Rambaut, 2014).

2.5.2. Maximum likelihood reconstructions

The sequential version of the Randomised Axelerated Maximum Likelihood (RAxML) package v.8.2.11 was used for all ML inferences of phylogeny (Stamatakis, 2014). Two different nucleotide substitution rate and site-specific evolutionary rate models were used for the three datasets. For the ITS2 data, the GTRCAT model was selected, while the GTRGAMMA model was utilised for both the *trnH-psbA* and *matK* sequences.

For each dataset, a total of 100 ML trees were generated on distinct starting trees, to obtain a single tree with the best likelihood in the first step of the analysis. Subsequently, the rapid bootstrapping algorithm was implemented, by selection of the 'autoMRE' bootstrap convergence criterion option. Finally, the bootstrapped replicate trees computed by the previous step were used to draw taxon bipartitions on the best ML tree retained in the first step (Lewis and Olmstead, 2001; Pattengale et al., 2010; Stamatakis, 2014). The final ML trees generated for each of the three datasets were then edited in the Dendroscope 3.5.7 (Huson et al., 2007) and FigTree v.1.4.2 (Rambaut, 2014) packages.

2.5.3. Evolutionary divergence calculations

For examination of the magnitudes of evolutionary divergence between species, net evolutionary divergence estimates were computed in MEGA6 (Tamura et al., 2013). Computations were carried out independently for each marker, all using the Tamura–Nei model (Tamura and Nei, 1993), involving 72, 77 and 82 nucleotide sequences for the ITS2, *trnH-psbA* and *matK* regions, respectively. No data was available for *S. isoetifolium* samples in the ITS2 region, as they all failed to amplify (see results).

Codon positions included for the *trnH-psbA* sequences were 1st + 2nd + 3rd + Noncoding, with all positions for all sequences containing less than 5% site coverage eliminated, i.e. fewer than 95% alignment gaps, missing data and ambiguous bases were allowed at any position. Totals of 350, 380 and 907 positions for the ITS2, *trnH-psbA* and *matK* regions, respectively, were retained in the final datasets for computation. Standard error estimates for each divergence value calculated were obtained following a bootstrap procedure involving 1000 replicates.

3. Results

3.1. Morphological analyses

Morphological trait analyses of leaves between *H. ovalis* and the endemic *H. ovalis* subsp. *bullosa* (Fig. 2) showed no significant differences. The leaf blades of *H. ovalis* and *H. ovalis* subsp. *bullosa* are grass green in colour, oval to oblong or paddle-like in shape with a rounded apex (Fig. 2B). In both taxa, a pair of leaves usually arise from a 10–45 mm long petiole. The leaves of *H. ovalis* and *H. ovalis* subsp. *bullosa* have six to ten pairs of pinnate cross veins, which join the intra-marginal veins. Similarly, the leaf margin is smooth throughout and lack hairs on the surface of both species. However, the leaf surface of *H. ovalis* lacks the blister-like or bullate indentations present on both sides of the leaf blade in *H. ovalis* subsp. *bullosa*. All Fijian specimens are small, with a slender, prostrate, branched, pale white rhizome 2 mm in diameter, which is either wiry and tough, or fragile and delicate, depending on the wave energy environment the plant is collected from. Morphological analyses of the collected *Halophila* samples indicate the material to be *H. ovalis*. The smooth-surfaced, paddle-shaped, paired leaves, without serrated leaf margins, are typical of *H. ovalis* (den Hartog, 1970; Short et al., 2010), and the female flowers and fruits were also consistent with this species (Fig. 2).

Vegetative and reproductive character comparisons between *H. ovalis* and the endemic *H. ovalis* subsp. *bullosa* are presented in Table 1. Moreover, *H. ovalis* subsp. *bullosa* have similar morphological characteristics to those previously described in the literature for *H. ovalis*, except for leaf surface texture and the number of seeds per fruit.

3.2. Phylogenetic inferences

3.2.1. Sequence alignments and substitution model testing

Following sequence editing and alignment, final nexus format files were generated for each marker type. Table 2 details the numbers of cleaned and aligned sequences retained for each species, for each respective marker type. Unfortunately, all *S. isoetifolium* samples failed to amplify for the ITS2 region, and therefore no sequences were available for this taxon/marker combination.

Substitution model selection tests implemented in jModelTest revealed differing model choices for each gene region, based on 14, 8, and 5 sequences tested for the ITS2, *trnH-psbA* and *matK* regions, respectively. The number of input sequences for model testing needed to be trimmed from the full datasets, as there

Fig. 2. *Halophila ovalis* subsp. *bullosa* from Fiji Islands; Clockwise from upper left: A – Female flower comprising an ovary, a hypanthium, three styles (scale bar = 1 mm). B - Leaf showing the tip and the mid-vein, bullated surface (scale bar = 1 cm). C- Male flower comprised of anther and shorter stalk (scale bar = 1 mm). D – Mature male flower showing anther and three tepals (scale bar = 1 mm). E - Fruit attached to rhizomes containing globose seeds enclosed by a testa with small peg like projection called hypanthium (scale bar = 1 mm). F- Seeds released from fruit (scale bar = 1 mm). Photographs: S. Singh. (For interpretation of the references to colour in this figure legend, the reader is referred to the web version of this article.)

Table 1
Comparison of vegetative and reproductive characters of *Halophila ovalis* from den Hartog (1970) with *Halophila ovalis* subsp. *bullosa* from Fiji. Bold print indicates characters lacking overlap with *H. ovalis*.

Parameters	Character comparison	
	Halophila ovalis den Hartog (1970) and Tuiwawa et al. (2014)	*Halophila ovalis* subsp. *bullosa* from Fiji present study (n = 15)
Vegetative morphology		
Rhizome internode length (mm)	10–50	15–30
Scale hairs	Absent	Absent
Petiole length (mm)	10–45	6–45
Leaf form	Oval-oblong	Oval-oblong
Leaf length (mm)	10–40	10–40
Leaf width (mm)	5–20	5–20
Leaf surface	**Smooth**	**Blister-like or bullate**
Leaf margins	Entire	Entire
Number of cross-veins	10–25	6–10
Reproductive morphology		
Flowering spathe hairs	Absent	Absent
Male flower	Known	Known
Female flower		
Ovary length (mm)	1–1.5	1–1.5
Style length (mm)	10–20	10–25
Seeds (numbers per fruit)	**20–30**	**7–12**

Table 2
Numbers of edited and aligned sequences retained for each gene region for each species.

Species	ITS2	*trnH-psbA*	*matK*
Halodule uninervis	18	20	20
Halodule pinifolia	20	20	20
Halophila ovalis	15	14	14
Halophila ovalis subsp. *bullosa*	19	18	20
Syringodium isoetifolium	0	5	8
Total number of sequences	**72**	**77**	**82**

is an upper limit to the number of sequences and characters jModelTest is able to accept.

The Hasegawa–Kishono–Yano (HKY) model was determined to have the best fit for the ITS2 data (-lnL = 849.45, BIC = 1876.47 and delta = 0.00), while for the *trnH-psbA* sequences, the HKY model with gamma-shaped rate variation (HKY+G) was found to be optimal (-lnL = 807.23, BIC = 1727.58 and delta = 0.00). For the *matK* data, the TPM1uf model (-lnL = 1876.11, BIC = 3840.75 and delta = 0.00) had the best fit.

3.2.2. Reconstructions

Bayesian and ML reconstructions generated using the ITS2 and *trnH-psbA* sequences are presented in Figs. 3 and 4, respectively. Reconstructions using the *matK* sequences produced nearly identical topologies to the *trnH-psbA* data, and therefore are not shown. For the ITS2 sequences, because all *S. isoetifolium* samples experienced amplification issues with this marker, *H. pinifolia* was selected as the outgroup. The remaining cpDNA markers included *S. isoetifolium* samples however, and therefore this taxon was chosen as the outgroup. Sequence quality data for all three markers is accessible under the BOLD system repository available online at http://www.boldsystems.org, under the project name "FSDNA Fiji Islands Seagrass DNA Barcoding".

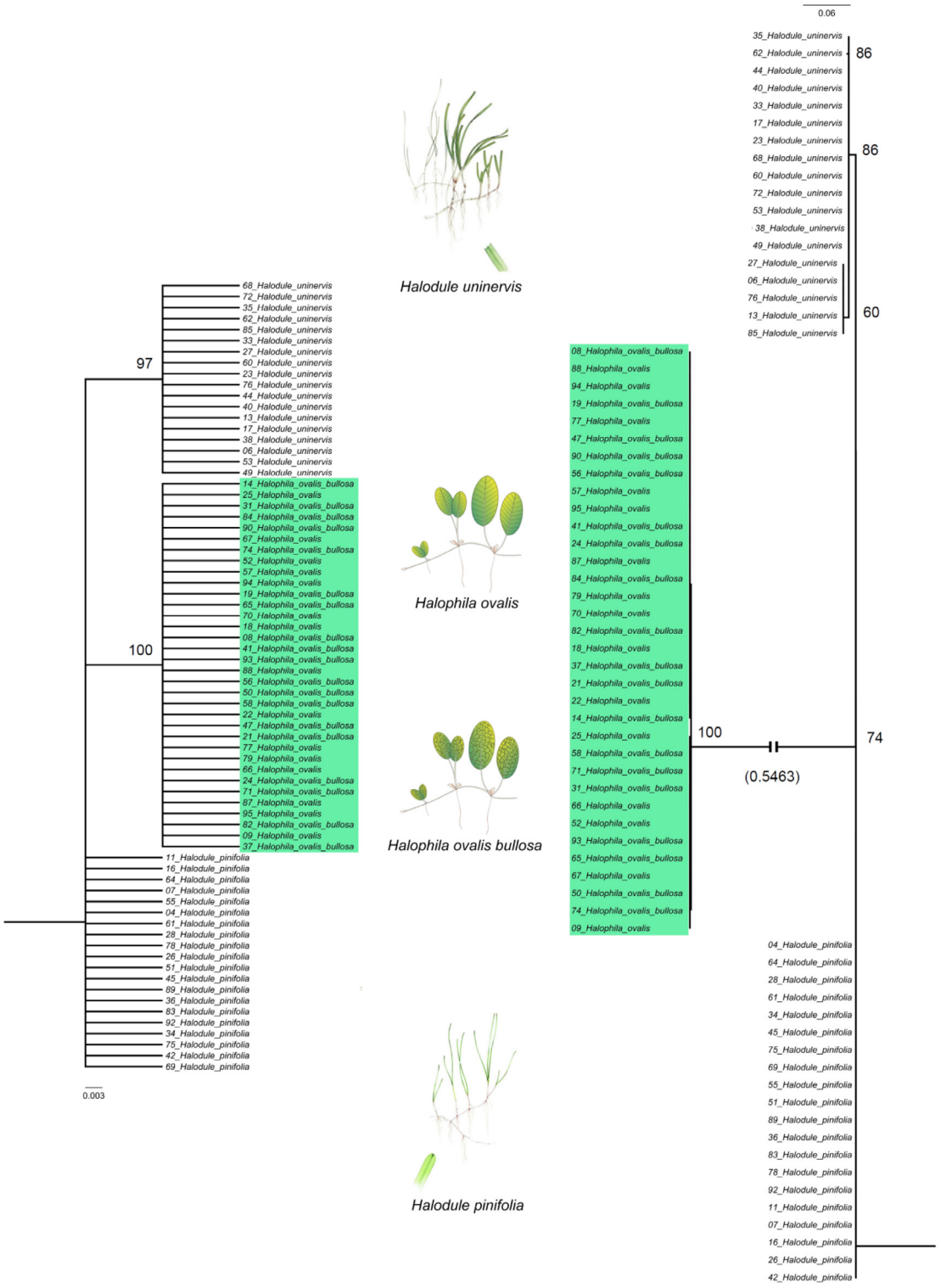

Fig. 3. Bayesian (left) and Maximum Likelihood (right) reconstructions based on 72 ITS2 nucleotide sequences. Bayesian inference (MrBayes) utilised the HKY model, while ML reconstruction (RAxML) was under the GTRGAMMA model. The Bayesian tree is a strict consensus of 169 highly credible trees (cumulative posterior P = 0.990). Node support values represent posterior probabilities for the Bayesian tree, while bootstrap values are presented on the ML tree. The branch length is presented in parentheses for the *H. ovalis*/*H. ovalis* subsp. *bullosa* clade, as the branch had to be truncated for presentation. The *H. ovalis*/*H. ovalis* subsp. *bullosa* clades on both trees have been highlighted in green, and for both trees, *H. pinifolia* was used as the outgroup. Scale bars represent the number of substitutions per site. [Image credit: http://www.seagrasswatch.org & http://www.supagro.fr]. (For interpretation of the references to colour in this figure legend, the reader is referred to the web version of this article.)

3.2.3. Bayesian and ML reconstructions

Bayesian reconstructions using the ITS2, *trnH-psbA* and *matK* sequences respectively, generated totals of 16002/20002; 4964/6204 and 4648/5808 trees which were sampled from both MrBayes runs. Following discard of the burn-in set (20%); 15,842, 4915 and 4602 credible trees remained for calculation of

posterior probabilities for each marker, respectively. The final average standard deviation of split frequencies achieved was 0.0033; 0.0048 and 0.0047 for the ITS2, *trnH-psbA* and *matK* datasets, respectively, with an average potential scale reduction factor (PSRF) for parameter values of 1.000 in all runs.

Within the final sets of credible trees, cut-off thresholds for individual tree and cumulative posterior probabilities resulted in 169, 102 and 96 highly credible trees being retained for the ITS2, *trnH-psbA* and *matK* datasets, respectively. Subsequently, consensus phylograms for each marker were generated, with differing clades/taxa being selected as outgroups.

Maximum Likelihood inferences recovered the most likely tree (highest likelihood score) during searches of the first 50 randomised trees generated during initial trial runs for all datasets. Therefore, all final runs were carried out specifying 100 trees to generate the best ML tree. The rapid automatic bootstrapping function using the Extended Majority Rules ('autoMRE') method converged for all datasets after applying less than 500 bootstraps.

3.2.4. Phylogenetic relationships

The Bayesian and ML reconstructions generated nearly identical relationships among the seagrass genera sampled across all three markers, with strong support for the monophyly of all *H. ovalis* and *H. ovalis* subsp. *bullosa* samples (Bayesian posterior probability node support and ML bootstrap values = 100).

Samples of *H. ovalis* and *H. ovalis* subsp. *bullosa* resolved as a monophyletic clade across the ITS2, *trnH-psbA* and *matK* datasets, with consistently short internal branch lengths among clade members. Individual monophyletic clades in all reconstructions were also resolved for *H. uninervis* and *H. pinifolia*, respectively, which are known to be sister-taxa. When trees were rooted with *S. isoetifolium* as the outgroup (which was possible only for the *trnH-psbA* and *matK* sequences), both *Halodule* taxa grouped together in a parallel branch to the *Halophila ovalis/ovalis* subsp. *bullosa* clade.

Both Bayesian and ML reconstructions using the two plastid markers revealed *H. uninervis* grouping in a basal clade to *H. pinifolia* (Fig. 3), while *S. isoetifolium* remained the most distantly related taxon to both *Halodule* and *Halophila*.

3.2.5. Evolutionary divergence estimates

Calculations of the net average estimate of base substitutions per site among and between taxa, strongly supported divergence patterns identified in the Bayesian and ML tree topologies (Table 3). Pairwise divergence estimates between *H. ovalis* and *H. ovalis* subsp. *bullosa* were zero for each of the ITS2, *trnH-psbA* and *matK* gene regions respectively, suggesting the conspecificity of these taxa. Low levels of divergence were also estimated between *H. uninervis* and *H. pinifolia*, with the ITS2 calculations producing the highest values (0.248 ± 0.408). Estimates at the two cpDNA markers were substantially lower however, being 0.011 ± 0.006 and 0.001 ± 0.001 for the *trnH-psbA* and *matK* loci, respectively, highlighting sensitivity differences between nrDNA and plastid gene regions.

The ITS2 sequences also produced the largest range of divergence estimates, from 0 (*H. ovalis* vs. *H. ovalis* subsp. *bullosa*) to 1.751 (*H. uninervis* vs. *H. ovalis*), while variation between the two cpDNA loci was smaller (e.g. *trnH-psbA* = 0.260 cf. *matK* = 0.198 for *H. uninervis* vs. *H. ovalis*; see Table 3). For all pairwise comparisons, *trnH-psbA* values were larger than those computed with *matK* sequences. Marked separation between *H. ovalis*/*H. ovalis* subsp. *bullosa* and *H. uninervis* with *H. pinifolia* was apparent only at the ITS2 locus, with pairwise estimates of 1.625 ± 0.293 and 1.751 ± 0.322 for *H. uninervis*, against *H. ovalis* subsp. *bullosa* and *H. ovalis*, respectively. Corresponding estimates for *H. pinifolia* were 1.220 ± 0.166 and 1.222 ± 0.169, against *H. ovalis* subsp. *bullosa* and *H. ovalis*, respectively. Divergence estimates at the *matK* locus were nearly identical, ranging from 0.200–0.198 (*H. uninervis* vs. *H. ovalis* subsp. *bullosa* and *H. ovalis*, respectively), cf. corresponding values of 0.198–0.197 for *H. pinifolia*. Similar patterns were evident for *trnH-psbA* sequences (Table 3).

Of all five taxa sampled, *S. isoetifolium* was found to be the most divergent, with pairwise estimates of 0.262 ± 0.039 and 0.268 ± 0.040 at the *trnH-psbA* locus when compared with *H. ovalis* subsp. *bullosa* and *H. ovalis* samples, respectively. Closer affinity with the two *Halodule* taxa was evident however, with estimates of 0.119 ± 0.021 and 0.133 ± 0.022 with *H. uninervis* and *H. pinifolia*, respectively. Similar patterns were apparent at the *matK* locus, and consistent with both Bayesian and ML tree topologies.

4. Discussion

This study used independent morphological and molecular barcoding approaches to determine if Fijian *H. ovalis* and *H. ovalis* subsp. *bullosa* are conspecific. Comparisons of morphological observations of both vegetative and floral structures of *H. ovalis* subsp. *bullosa* to characteristics described and observed in *H. ovalis,* showed only minor differences, principally for the leaf surface type and number of seeds per fruits. These differences however, were within the ranges described for *H. ovalis*, making the taxa indistinguishable on the basis of morphology alone. Molecular phylogenetic reconstructions using two independent gene regions resolved one clade comprising *H. ovalis* and *H. ovalis* subsp. *bullosa*, confirming their conspecificity.

4.1. Molecular barcoding in seagrasses and examination of H. ovalis

Short et al. (2011) recently suggested that taxa should be accepted as new species only if a complete published taxonomic description exists, documenting unique sexual reproductive characters and significant genetic differences. However, there is no general agreement on the recommended DNA barcoding approach to be used for seagrasses (Lucas et al., 2012). Hence, previous molecular analyses of other seagrass and plant taxa (Kuzmina et al., 2017; Kuzmina and Ivanova, 2011a,b; Waycott et al., 2002, 2006) were used for selection of the nuclear (ITS) and chloroplast markers (*trnH-psbA* and *matK*) for the current study.

Using phylogenetic reconstructions, both nuclear and chloroplast markers showed that the specimens identified as *H. ovalis* subsp. *bullosa* belong to the same clade as *H. ovalis*. In addition, both phylogenetic trees (Bayesian and ML methods), plus pairwise estimations of evolutionary divergence support the monophyly of *H. ovalis* and *H. ovalis* subsp. *bullosa*. Thus, the endemic *H. ovalis* subsp. *bullosa* recognised in Fiji as a subspecies (Skelton and South, 2006; Tuiwawa et al., 2014), is not separable from *H. ovalis* at both nuclear (ITS2) and chloroplast markers (*trnH-psbA* and *matK*), and are in fact conspecific. This position is also supported by morphological data provided in the current study.

Results of the current study indicate that the ITS, *trnH-psbA* and *matK* regions are useful at differentiating within *Halophila* taxa, and are likely to be informative for investigating taxonomic relationships within other seagrass genera, or indeed other aquatic plant taxa. Overall, our results support the conclusion of Waycott et al. (2002) for a critical taxonomic revision of the genus *Halophila*, and mandate a merger between the endemic *H. ovalis* subsp. *bullosa* and *H. ovalis* for the Fiji Islands.

Table 3
Pairwise estimates of net evolutionary divergence between species. The number of base substitutions per site, from estimation of the net average between groups of sequences is shown in order for the ITS2, *trnH-psbA* and *matK* gene regions respectively, from top to bottom, below the diagonal. Standard error estimates are shown above the diagonal in blue.

Species	*Syringodium isoetifolium*	*Halophila ovalis* subsp. *bullosa*	*Halophila ovalis*	*Halodule uninervis*	*Halodule pinifolia*
		-	-	-	-
Syringodium isoetifolium		0.039	0.040	0.021	0.022
		0.018	0.018	0.009	0.009
	-		0.002	0.293	0.166
Halophila ovalis	0.262		0.000	0.038	0.037
subsp. *bullosa*	0.205		0.000	0.018	0.018
	-	0.000		0.322	0.169
Halophila	0.268	0.000		0.038	0.038
ovalis	0.204	0.000		0.018	0.018
	-	1.625	1.751		0.408
	0.119	0.255	0.260		0.006
Halodule uninervis	0.070	0.200	0.198		0.001
	-	1.220	1.222	0.248	
Halodule	0.133	0.248	0.253	0.011	
pinifolia	0.068	0.198	0.197	0.001	

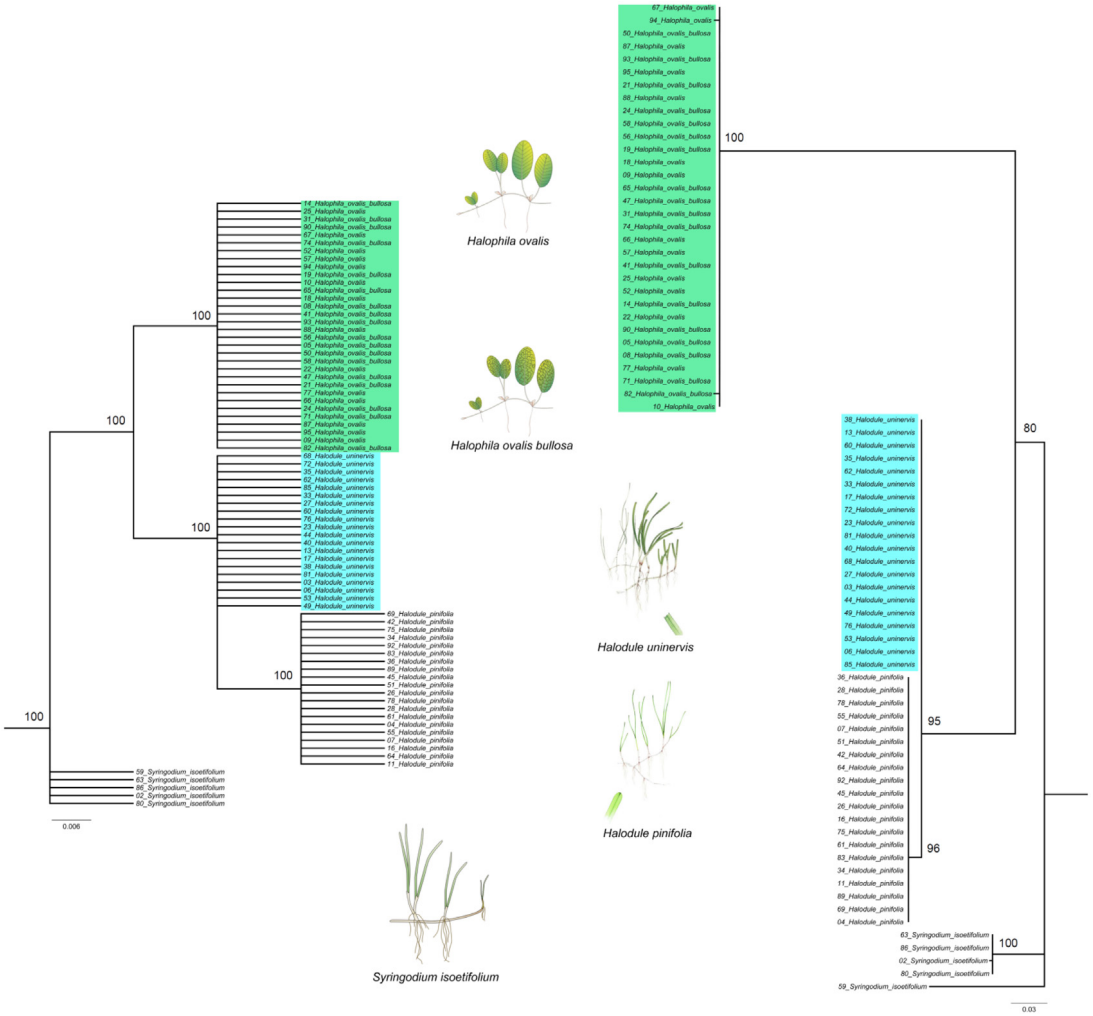

Fig. 4. Bayesian (left) and Maximum Likelihood (right) reconstructions based on 77 *trnH-psbA* nucleotide sequences. Bayesian inference (MrBayes) utilised the HKY+G model, while ML reconstruction (RAxML) was under the GTRGAMMA model. The Bayesian tree is a strict consensus of 102 highly credible trees (cumulative posterior P = 0.980). Node support values represent posterior probabilities for the Bayesian tree, while bootstrap values are presented on the ML tree. The *H. ovalis*/*ovalis* subsp. *bullosa* clades on both trees have been highlighted in green, while *H. uninervis* clades are highlighted in blue. For both trees, *S. isoetifolium* was used as the outgroup. Scale bars represent the number of substitutions per site. [Image credit: http://www.seagrasswatch.org & http://www.supagro.fr]. (For interpretation of the references to colour in this figure legend, the reader is referred to the web version of this article.)

4.2. Morphological insights

Reproductive material from both *H. ovalis* and *H. ovalis* subsp. *bullosa* showed identical female and male reproductive parts (pers. obs., Fig. 2). Some small differences in plant morphology were found between the species descriptors of *H. ovalis* (den Hartog, 1970; Tuiwawa et al., 2014), and samples of *H. ovalis* subsp. *bullosa* (Table 1). These differences occur on the leaf surface as blister-like or bullate indentations on both sides of the blade, and the number of seeds per fruit being between 7–12 seeds (cf. up to 30 seeds per fruit for *H. ovalis*). Additionally, the leaf surface bullation feature of *H. ovalis* subsp. *bullosa* (Fig. 2B) is not reported for *H. ovalis* (den Hartog, 1970; Tuiwawa et al., 2014), but leaf morphology variations have been reported in some widespread populations of *H. ovalis* from Egypt, Thailand, China, Guam and the Philippines (Short et al., 2010). Overall, the morphological characteristics of *H. ovalis* subsp. *bullosa* are remarkably similar to *H. ovalis*, especially the male and female flowers described in literature. Likewise, during field collections of *H. ovalis* specimens, smooth and bullated leaves were at some locations found to be present on the same plant, and similarly population dominance of both species fluctuated seasonally in the same locations (Shalini Singh, *pers. obs*).

4.3. Halophila relationships and phenotypic plasticity

Species within the genus *Halophila* have long been recognised for variation of leaf morphology relating to shape, texture, colour and blade size. This is particularly the case for *H. ovalis* (Short et al., 2007; Hedge et al., 2009; Nguyen et al., 2014), *H. hawaiana* (McDermid et al., 2003), and *H. nipponica* (Shimada et al., 2012). The application of traditional classification methods, largely based on leaf morphology, has often been challenging, and misidentification of species has caused disagreement among seagrass taxonomists (Short et al., 2011; Shimada et al., 2012; Nguyen et al., 2014). Conversely, molecular markers were found to have higher discriminatory power between *Halophila* species, especially at nuclear markers e.g. ITS (Nguyen et al., 2014), and the chloroplast markers *trnH-psbA* and *matK* reported by Nguyen et al. (2013) and Lucas et al. (2012).

Among the *H. ovalis* and *H. ovalis* subsp. *bullosa* samples examined here, the lack of DNA sequence variation and their resolution as a monophyletic clade despite subtle morphological differences, supports the notion that affiliates of this group are either very closely related, or actually the same taxon. This notion agrees with the conclusions of Waycott et al. (2002). Furthermore, McMillan and Bridges (1982) who investigated *Halophila* samples possessing smooth and bullated leaves on different individual plants from both Fiji and Samoa, reported identical isozyme patterns for five enzyme systems. In addition, culture experiments on plants from both Fiji and Samoa, observed that environmental manipulations can induce bullated or smooth leaved plants (Skelton and South, 2006).

The apparent plastic leaf phenotype of *H. ovalis* subsp. *bullosa* may be influenced by environmental conditions, as demonstrated in various *Halophila* species reported by McDermid et al. (2003). Suggestions for the monophyly of *H. ovalis* are not new, as morphological diversity in a species may be accompanied by genetic diversity. Consequently, Waycott et al. (2002) considered *H. ovalis* to be a complex of closely related individuals, whose leaves are highly plastic, especially in relation to blade size, shape, colour and texture (McKenzie and Yoshida, 2007).

Despite this suggestion, several morphologically distinct taxa are also recognised e.g. *H. hawaiiana*, *H. johnsonii*, *H. ovata* and *H. minor*. Moreover, Short et al. (2010) concluded that the *H. ovalis* species complex contains little variation (genetic divergences ranging from 0–0.016% between *H. ovalis* from Antigua, cf. *H. ovalis/johnsonii/hawaiiana* from Indonesia, Florida and Vietnam, respectively), but wide morphological plasticity. In addition, Papenbrock (2012) stated that *Halophila* species exhibit various degrees of morphological variation depending on habitat and reproduction. Similarly, Bricker et al. (2011) suggested that phenotypic plasticity could be an underestimated trait for seagrasses, enabling survival in different niches such as intertidal areas, shallow turbid waters, light limited areas and deep waters (Lucas et al., 2012).

5. Conclusion

Results of this study indicate that the vegetative and reproductive morphology of *Halophila ovalis* subsp. *bullosa* falls within the bounds of what has been reported for *Halophila ovalis*, despite small differences in certain character counts. Parallel phylogenetic analyses also confirm the common taxonomic identity of Fijian *Halophila ovalis* and *H. ovalis* subsp. *bullosa* material, supporting revision and merger recommendations of this species and subspecies, as they may have been misidentified. The findings described here while applied for resolving the taxonomic identity of a Fijian seagrass, may also be useful for resolving relationships in other seagrass taxa, with the use of a joint morphological-molecular barcoding approach. Such an approach is important for describing diversity and distribution in seagrasses and other aquatic plants, and has high utility for informing global conservation and management efforts.

Acknowledgements

We are deeply indebted to Maria Kuzmina, Centre for Biodiversity Genomics, University of Guelph, Ontario, Canada, for help with DNA lab analysis. We also thank aquaculture staff at the Marine Studies Programme, University of the South Pacific, for their kind support in the laboratory work. We like to thank Gilianne Brodie for collection of sample from Vanua Levu. Thank you to Antione N'Yeurt for his assistance and support in the research. We also thank the anonymous reviewers whose comments have improved the quality of this manuscript. This research was financially supported by the Pacific Centre for Environment and Sustainable Development, University of the South Pacific, Fiji.

Appendix A. Supplementary data

Supplementary material related to this article can be found online at https://doi.org/10.1016/j.rsma.2019.100809.

References

Bricker, E., Waycott, M., Calladine, A., Zieman, J.C., 2011. High connectivity across environmental gradients and implications for phenotypic plasticity in a marine plant. Mar. Ecol. Prog. Ser. 423, 57–67.

Chen, S., Yao, H., Han, J., Liu, C., Song, J., Shi, L., Zhu, Y., Ma, X., Gao, T., Pang, X., Luo, K., Li, Y., Li, X., Jia, X., Lin, Y., Leon, C., 2010. Validation of the ITS2 region as a novel DNA barcode for identifying medicinal plant species. PLoS One 5, e8613.

Cowart, D.A., Pinheiro, M., Mouchel, O., Maguer, M., Grall, J., Miné, J., Amaud-Haond, S., 2015. Metabarcoding is powerful yet still blind: a comparative analysis of morphological and molecular surveys of seagrass communities. PLoS One 10 (2), e0117562. http://dx.doi.org/10.1371/journal.pone.0117562.

Dunning, L.T., Savolainen, V., 2010. Broad-scale amplification of *matK* For DNA barcoding plants, a technical note. Bot. J. Linn. Soc. 164, 1–9.

Edgar, R.C., 2004. MUSCLE: multiple sequence alignment with high accuracy and high throughput. Nucl. Acids Res. 32, 1792–1797.

Ford, C.S., Ayres, K.L., Toomey, N., Haider, N., Stahl, J.V., 2009. Selection of candidate coding DNA barcoding regions for use on land plants. Bot. J. Linn. Soc. 159, 1–11.

den Hartog, C., 1970. The Sea-Grasses of the World. North-Holland, Amsterdam.

den Hartog, C., Kuo, J., 2006. Taxonomy and biogeography of seagrasses. In: den Hartog, C., Kuo, J., Larkum, A., Orth, R., Duarte, C. (Eds.), Seagrasses: Biology, Ecology and Conservation. Springer, pp. 1–23.

Hedge, S., Smith, N., Unsworth, R.K.F., 2009. Temporal and spatial morphological variability of the seagrasses *Halophila ovalis* and *Halodule uninervis* throughout the Great Barrier reef region: preliminary analysis, report to the marine and tropical sciences research facility. Cairns: reef and rainforest research centre limited.

Huelsenbeck, J.P., Ronquist, F., 2001. MRBAYES: Bayesian inference of phylogenetic trees. Bioinformatics 17, 754–755.

Huson, D.H., Richter, D.C., Rausch, C., Dezulian, T., Franz, M., Rupp, R., 2007. Dendroscope: an interactive viewer for large phylogenetic trees. BMC Bioinformatics 8, 1–6.

Ivanova, N.V., Dewaard, J.R., Hebert, P.D.N., 2006. An inexpensive, automation-friendly protocol for recovering high-quality DNA. Mol. Ecol. Notes 6, 998–1002.

Ivanova, N.V., Fazekas, A.J., Hebert, P.D.N., 2008. Semi-automated, membrane-based protocol for DNA isolation from plants. Plant Mol. Biol. Rep. 26 (186).

Ji, Y., Ashton, L., Pedley, S.M., Edwards, D.P., Tang, Y., Nakamura, A., Kitching, R., Dolman, P.M., Woodcock, P., Edwards, F.A., Larsen, T.H., Hsu, W.W., Benedick, S., Harver, K.C., Wilcove, D.S., Bruce, C., Wang, X., Levi, T., Lott, M., Emerson, B.C., Yu, D.W., 2013. Reliable, verifiable and efficient monitoring of biodiversity via metabarcoding. Ecol. Lett. 16, 1245–1257. http://dx.doi.org/10.1111/ele.12162, PMID: 23910579.

Kim, Y.K., Kim, S.H., Yi, J.M., Kang, C.K., Short, F., Lee, K.S., 2017. Genetic identification and evolutionary trends of the seagrass *Halophila nipponica* in temperate coastal waters of Korea. PLoS One 12 (5), e0177772. http://dx.doi.org/10.1371/journal.pone.0177772.

Kimura, M., 1981. Estimation of evolutionary distances between homologous nucleotide sequences. Proc. Natl. Acad. Sci. 78, 454.

Kuo, J., Kanamoto, Z., Iizumi, H., Mukai, H., 2006. Seagrasses of the genus Halophila Thoars (Hydrocharitaceae) from Japan. Acta Phytotax. et Geobot. 57, 127–154.

Kuzmina, M.L., Braukmann, T.W.A., Fazekas, A.J., Graham, S.W., Dewaard, S.L., Rodrigues, A., Bennett, B.A., Dickinson, T.A., Saarela, J.M., Catling, P.M., Newmaster, S.G., Percy, D.M., Fenneman, E., Moreau-Lauron, A., Ford, B., Gillespie, L., Subramanyam, R., Whitton, J., Jennings, L., Metsger, D., Warne, C.P., Brown, A., Sears, E., Dewaard, J.R., Zakharov, E.V., Herbert, P.D.N., 2017. Using herbarium-derived DNAs to assemble a large-scale DNA barcode library for the vascular plants of Canada. Appl. Plant Sci. 5 (12), 1700079.

Kuzmina, M.L., Ivanova, N.V., 2011a. Canadian Centre for DNA Barcoding protocols: PCR amplification for plants and fungi. http://ccdb.ca/site/wp-content/uploads/2016/09/CCDB_Amplification-Plants.pdf [accessed 14.11.17].

Kuzmina, M.L., Ivanova, N.V., 2011b. Canadian Centre for DNA Barcoding protocols: primer sets for plants and fungi, p. 3 [accessed 14.11.17].

Lal, M.M., Southgate, P.C., Jerry, D.R., Bosserelle, C., Zenger, K.R., 2016. A parallel population genomic and hydrodynamic approach to fishery management of highly-dispersive marine invertebrates: the case of the Fijian black-lip pearl oyster *Pinctada margaritifera*. PLoS One 11 (8), e0161390. http://dx.doi.org/10.1371/journal.pone.0161390.

Lecocq, T., Vereecken, N.J., Michez, D., Dellicour, S., Lhomme, P., Valterova, I., Rasplus, J.-Y., Rasmont, P., 2013. Patterns of genetic and reproductive traits differentiation in mainland vs. Corsican populations of bumblebees. PLoS One 8, e65642. http://dx.doi.org/10.1371/journal.pone.0065642.

Lewis, P.O., Olmstead, R., 2001. A likelihood approach to estimating phylogeny from discrete morphological character data. Syst. Biol. 50, 913–925.

Lucas, C., Tangaradjou, T., Papenbrock, J., 2012. Development of a DNA barcoding system for seagrasses: successful but not simple. PLoS One 7 (1), e29987.

Maxwell, P.S., Pitt, K.A., Burfeind, D.D., Olds, A.D., Babcock, R.C., Connolly, R.M., 2014. Phenotypic plasticity promotes persistence following severe events: physiological and morphological responses of seagrass to flooding. J. Ecol. 102, 54–64.

McDermid, K.J., Gregoritza, M.C., Reeves, J.W., Freshwater, D.W., 2003. Morphological and genetic variation in the endemic seagrass *Halophila hawaiiana* (Hydrocharitaceae) in the Hawaiian Archipelago. Pac. Sci. 57 (2), 199–209.

McDonald, A.M., Prado, P., Heck, K.L., Fourqurean, J.W., Frankovich, T.A., Dunton, K.H., Cebrian, J., 2016. Seagrass growth, reproductive, and morphological plasticity across environmental gradients over a large spatial scale. Aquat. Bot. 134, 87–96.

McKenzie, L.J., Yoshida, R.L., 2007. Seagrass-watch: guidelines for monitoring seagrass habitats in the Fiji Islands. In: Proceedings of a Training Workshop, Corpus Christic Teachers' College, Laucala Bay, Suva, Fiji, 16 June, 2007 (Seagrass-Watch HQ, Cairns). p. 42.

McMillan, C., Bridges, K.W., 1982. Systematic implications of bullate leaves and isozymes for *Halophila* from Fiji and Western Samoa. Aquat. Bot. 12, 173–188.

Nguyen, X.V., Bujang, J.S., Papenbrock, J., 2013. Variability of leaf morphology and marker genes of members of the *Halophila* complex collected in Viet Nam. Aquat. Bot. 110, 6–15.

Nguyen, V.X., Detcharoen, M., Tuntiprapas, P., Soe-Htun, U., Sidik, J.B., Harah, M.Z., Prathep, A., Papenbrock, J., 2014. Genetic species identification and population structure of *Halophila* (Hydrocharitaceae) from the Western Pacific to the Eastern Indian Ocean. BMC Evol. Biol. 14, 1–18.

Papenbrock, J., 2012. Highlights in Seagrasses' phylogeny, physiology, and metabolism: what makes them special? Int. Sch. Res. Netw. Bot. 1–15.

Pattengale, N.D., Alipour, M., Bininda-Emonds, O.R.P., Moret, B.M.E., Stamatakis, A., 2010. How many bootstrap replicates are necessary? J. Comput. Biol. 17, 337–354.

Posada, D., 2008. JModelTest: phylogenetic model averaging. Mol. Biol. Evol. 25, 1253–1256.

Rambaut, A., 2014. FigTree v.1.4.2: tree drawing tool. Andrew Rambaut. http://tree.bio.ed.ac.uk/software/figtree/.

Rambaut, A., Suchard, M., Drummond, A.J., 2003. Tracer v.1.6. http://tree.bio.ed.ac.uk/software/tracer/.

Ratnasingham, S., Hebert, P.D.N., 2007. Bold: the barcode of life data system. Mol. Ecol. Notes 7, 355–364, (http://www.barcodinglife.org).

Ratnasingham, S., Hebert, P.D.N., 2013. A DNA-based registry for all animal species: the barcode index number (BIN) system. PLoS One 8, e66213.

Ronquist, F., Huelsenbeck, J.P., 2003. MrBayes 3: Bayesian phylogenetic inference under mixed models. Bioinformatics 19, 1572–1574.

Ronquist, F., Teslenko, M., van der Mark, P., Ayres, D.L., Darling, A., Hohna, S., Larget, B., Liu, L., Suchard, M.A., Huelsenbeck, J.P., 2012. MrBayes 3.2: efficient Bayesian phylogenetic inference and model choice across a large model space. Syst. Biol. 61, 539–542.

Sang, T., Crawford, D.J., Stuessy, T.F., 1997. Chloroplast DNA phylogeny, reticulate evolution, and biogeography of *Paeonia* (Paeoniaceae). Am. J. Bot. 84, 1120–1136.

Shimada, S., Watanabe, M., Ichihara, K., Uchimura, U., 2012. Morphological variations of seagrass species, *Halophila nipponica* (Hydrocharitaceae, Alismatales). Coast Mar. Sci. 35, 85–90.

Short, F., Carruthers, T., Dennison, W., Waycott, M., 2007. Global seagrass distribution and diversity: a bioregional model. J. Exp. Mar. Biol. Ecol. 350, 3–20.

Short, F.T., Moore, G.E., Peyton, K.A., 2010. *Halophila ovalis* in the tropical Atlantic Ocean. Aquat. Bot. 93, 141–146.

Short, F.T., Polidoro, B., Livingstone, S.R., Carpenter, K.E., Bandeira, S., Bujang, J.S., Calumpong, H.P., Carruthers, T.J.B., Coles, R.G., Dennison, W.C., Erftemeijer, P.L.A., Fortes, M.D., Freeman, A.S., Jagtap, T.G., Kamal, A.H.M., Kendrick, G.A., Kenworthy, W.J., LaNafie, Y.A., Nasution, I.M., Orth, R.J., Prathep, A., Sanciangco, J.C., Tussenbroek, B.V., Vergara, S.G., Waycott, M., Zieman, J.C., 2011. Extinction risk assessment of the world's seagrass species. Biol. Cons. 144, 1961–1971.

Skelton, P.A., South, G.R., 2006. Seagrass biodiversity of the Fiji and Samoa islands. South Pac. New Zeal. J. Mar. Fresh. 40, 345–356.

Stamatakis, A., 2014. RAxML version 8: a tool for phylogenetic analysis and post-analysis of large phylogenies. Bioinformatics 30 (9), 1312–1313.

Tamura, K., Nei, M., 1993. Estimation of the number of nucleotide substitutions in the control region of mitochondrial DNA in humans and chimpanzees. Mol. Biol. Evol. 10, 512–526.

Tamura, K., Stecher, G., Peterson, D., Filipski, A., Kumar, S., 2013. MEGA6: molecular evolutionary genetics analysis version 6.0. Mol. Biol. Evol. 30 (12), 2725–2729.

Tate, J.A., Simpson, B.B., 2003. Paraphyly of *Tarasa* (Malvaceae) and diverse origins of the polyploidy species. Syst. Bot. 28, 723–737.

Trivedi, S., Aloufi, A.A., Ansari, A.A., Ghosh, S.K., 2016. Role of DNA barcoding in marine biodiversity assessment and conservation: an update. Saudi J. Biol. Sci. 23, 161–171.

Tuiwawa, S., Skelton, P., Tuiwawa, M., 2014. A Field Guide to the Mangrove and Seagrass Species of Fiji. University of the South Pacific Press, Suva, Fiji Islands.

Vanitha, K., Subhashini, P., Thangaradjou, S.T., 2016. Karyomorphometric analysis of somatic chromosomes of selected seagrasses of families Hydrocharitaceae and Cymodoceaceae. Aquat. Bot. 133, 45–49.

Waycott, M., Freshwater, D.W., York, R.A., Calladine, A., Kenworthy, W.J., 2002. Evolutionary trends in the seagrass genus *Halophila* (Thouars): insights from molecular phylogeny. Bull. Mar. Sci. 71, 1299–1308.

Waycott, M., Procaccini, G., Les, D.H., Reusch, T.B.H., 2006. Seagrass evolution, ecology and conservation: a genetic perspective. In: den Hartog, C., Kuo, J., Larkum, A., Orth, R., Duarte, C. (Eds.), Seagrasses: Biology, Ecology and Conservation. Springer, pp. 25–50.

White, T.J., Bruns, T.D., Lee, S.B., Taylor, J.W., 1990. Amplification and direct sequencing of fungal ribosomal RNA genes for phylogenetics. In: Innis, M.A., Gelfand, D.H., Sninsky, J.J., White, T.J. (Eds.), PCR-Protocols and Applications - A Laboratory Manual. Academic Press, Cambridge, pp. 315–322.

Whitlock, R., Hipperson, H., Mannarelli, M., Burke, T., 2008. A high-throughput protocol for extracting high-purity genomic DNA from plants and animals. Mol. Ecol. Resour. 8, 736–741.